

Cite this: *J. Mater. Chem. C*, 2015,  
3, 8329

## Flexible copper wires through galvanic replacement of zinc paste: a highly cost-effective technology for wiring flexible printed circuits†

Jingping Liu,<sup>a</sup> Cheng Yang,<sup>\*a</sup> Peichao Zou,<sup>a</sup> Rui Yang,<sup>a</sup> Chao Xu,<sup>a</sup> Binghe Xie,<sup>a</sup>  
Ziyin Lin,<sup>b</sup> Feiyu Kang<sup>ac</sup> and Ching Ping Wong<sup>bd</sup>

Conventional electronic circuit wiring methods involve subtractive processes such as etching the copper foils, and thus are inefficient and cause serious environmental problems. Printed electronics technology is expected to be more environmentally benign and have lower cost, due to its additive characteristics. In this paper, we present a simple and efficient strategy to fabricate high performance copper metal fine circuits by a galvanic replacement deposition method. Zinc nanoparticles filled epoxy resin paste is printed onto the substrate film as the seed layer; with a subsequent simple galvanic replacement reaction between Zn and Cu<sup>2+</sup>, we can obtain a conductive Cu layer that can be further thickened by electroplating. The as-prepared circuits show bulk Cu conductivity, excellent flexibility, adhesion strength and pattern resolution. By adjusting the processing parameters, this technology is suitable for various practical applications, such as flexible circuit boards, RFID tags, touch panels, membrane switches, and photovoltaics, making it a promising solution for low-cost and environmentally friendly fabrication for flexible electronic devices.

Received 19th May 2015,  
Accepted 5th July 2015

DOI: 10.1039/c5tc01421b

www.rsc.org/MaterialsC

### Introduction

The last decade has seen explosive growth of flexible printed circuits and devices, such as large area displays, radio frequency identification (RFID),<sup>1,2</sup> sensors,<sup>3,4</sup> wearable electronic devices,<sup>5,6</sup> photovoltaic devices,<sup>7</sup> smart cards and energy storage devices<sup>8</sup> *etc.* Printed electronics technologies, *e.g.* inkjet printing,<sup>9,10</sup> screen printing,<sup>11,12</sup> gravure printing,<sup>13,14</sup> transfer printing,<sup>15–17</sup> micro-contact printing,<sup>18</sup> and 3D printing<sup>19,20</sup> *etc.*, as dry and additive fabrication technologies, provide efficient and inexpensive alternatives for the increasing demands of flexible electronics. In comparison, conventional wet and subtractive fabrication technologies, such as copper/aluminum etching processes have long been accused to be expensive, complicated processes, with low productivity, high energy consumption

characteristics which require the involvement of large volumes of hazardous waste.<sup>21,22</sup>

However, in cases where high conductivity is required, the available pure additive wiring technologies still have limitations. For example, solution based conductive inks that contain metal nanoparticles (Ag, Au, and Ni *etc.*) have been used for inkjet printing processes; the metal nanoparticles can be printed into desirable patterns and subsequently sintered at relatively low temperatures to achieve high conductivities.<sup>23,24</sup> Yet a low viscosity of the conductive ink is necessary for inkjet printing, which often involves volatile organic chemicals (VOCs). Additionally, multiple printing cycles are needed to ensure adequate wiring thickness so as to reduce electrical resistance and reduce losses.<sup>25</sup> Besides, the high material cost of the commonly used Au and Ag conductive fillers is another limitation for wider applications. When compared, screen printing, gravure printing, and offset printing *etc.* seem to be more cost-effective and environmentally benign.<sup>25,26</sup> Even though conductive pastes/adhesives have been widely used in the printing electronics technology, Ag pastes, for example, can only reach a conductivity of  $\sim 1 \times 10^5$  S cm<sup>-1</sup> even with a high filler loading of 80 wt%, which is about six times lower than bulk silver and is much more expensive than wiring copper.<sup>26</sup>

Copper (Cu) has long been regarded as the most promising wiring material because it has comparable conductivity to silver while it's about eighty times cheaper.<sup>27</sup> Recent technological advances are mainly focused on the rapid printing and sintering

<sup>a</sup> Division of Energy and Environment, Graduate School at Shenzhen, Tsinghua University, Shenzhen 518055, P. R. China.

E-mail: yang.cheng@sz.tsinghua.edu.cn

<sup>b</sup> School of Materials Science and Engineering, Georgia Institute of Technology, 771 Ferst Dr., Atlanta, GA 30332, USA

<sup>c</sup> School of Materials Science and Engineering, Tsinghua University, Beijing 100084, China

<sup>d</sup> Department of Electronic Engineering, The Chinese University of Hong Kong, Hong Kong, China

† Electronic supplementary information (ESI) available: Details of the Cu<sup>2+</sup> solutions, the electroplating conditions, the FTIR and DSC-TGA information for the epoxy resin and the Zn-epoxy paste, the lap-shear test and elemental analysis of the p-Cu samples, and the RFID tests. See DOI: 10.1039/c5tc01421b

technology for copper nanoparticle based conductive inks,<sup>25</sup> such as non-thermal or local surface thermal sintering examples,<sup>28–30</sup> which aim to provide lower production costs and better performances. But the poor oxidation resistance of Cu nanoparticles has been a great challenge for wider applications of the copper conductive inks.

An alternative route for wiring Cu-based circuits at low temperature is through electroless plating. The general process of electroless plating involves surface activation by seeding catalytic metal materials on the surface of the substrate to deposit copper on the activated surfaces in an electroless plating bath. By a printing process, such as inkjet printing<sup>31</sup> and micro-contact printing,<sup>32</sup> one can print the catalytic seed layer on the substrate and create Cu film patterns selectively on the seed layer. The palladium (Pd) catalyst is the most widely used material due to its high catalytic activity for the initiation of various metal deposition from a wide range of electroless plating baths.<sup>33</sup> Other catalysts or seed materials, such as copper salts/nanoparticles,<sup>34</sup> silver salts/nanoparticles<sup>35</sup> and poly(dopamine)<sup>36</sup> have also been investigated for their lower cost and less polluting characteristics compared with the Pd method. However, the cost of the materials, the substrate-dependent adhesion of the catalytic inks and the involvement of hazardous reducing agents are still challenging.<sup>37,38</sup>

In order to develop highly electrically conductive, low-cost, oxygen resistant and environmentally friendly copper wires by a simple and effective printing technology, herein we demonstrate an effective technology by using zinc (Zn) paste to act as the seed layer which can reduce the Cu<sup>2+</sup> ions into a continuous Cu layer at room temperature. By mixing Zn nano-powder with epoxy resin, this Zn paste can be printed by screen printing techniques *etc.*, whereby the Zn seed particles can be firmly adhered on various kinds of substrates *e.g.* FR4, polyimide (PI) films, poly(ethylene terephthalate) (PET) films and glass boards. Through a galvanic replacement reaction process, a conductive Cu layer can be deposited on the printed Zn patterns. With the subsequent Cu electro-plating process, we can obtain a bulk Cu layer with a thickness of up to 30 μm. In this way, we can create a highly conductive copper layer with a wiring resolution of 100 μm, which can be used for general flexible printed circuit (FPC) applications. The circuits show reliable performance and excellent electrical conductivity, mechanical flexibility, foldability, and adhesion strength to the substrates. Additionally, this technology can be conveniently scaled-up to roll-to-roll production.

## Experimental

### Zn-epoxy paste and Cu<sup>2+</sup> solution

The Zn paste for screen printing was composed of Zn nanoparticles with a size of 50 nm (Beijing Dk Nano technology Co., Ltd) and epoxy resin (Epon 828, Shell), curing agent (methyltetrahydrophthalic anhydride, MTHPA, Nanya Resins), and catalyst (hexamethylenetetramine (99%), Guangzhou Chemical Reagent Factory). The mixing of the resin binder was according to the equal epoxide equivalent weight (EEW) of the epoxy resin

and the hydroxyl equivalent weight (HEW) of the curing agent. A small amount of catalyst was added to the resin dispersant to accelerate crosslinking. The Zn loading percentage was 65 wt%. The Zn nanoparticles and resin were mixed with a planetary mixer (HASAI, HM1000) at 800 rpm for 30 min to form the homogeneous Zn paste. The as-prepared Zn paste was degassed under vacuum before use.

CuSO<sub>4</sub>·5H<sub>2</sub>O (AR, Aladdin) and poly(ethylene glycol) (PEG), (*M<sub>w</sub>*: 4000, AR, Aladdin) were selected as the Cu<sup>2+</sup> source and stabilizer. 23.4 g CuSO<sub>4</sub>·5H<sub>2</sub>O and 23.4 mg PEG4000 were added to 76.6 mL deionized (DI) water (100 g in total). The pH value was adjusted to 1.5 by using H<sub>2</sub>SO<sub>4</sub> before use.

### Galvanic replacement deposition of Cu conductive layer and electro-plating thick Cu layer

The Zn seed paste was screen printed onto a PET or PI film, and then the samples were cured at 150 °C for 20 min. The galvanic replacement reaction was conducted by immersing the samples into the as-prepared Cu<sup>2+</sup> source solution for 20 min. Then the samples were washed with DI water and dried in an oven (Memmert).

In order to obtain a thicker copper layer, an electroplating process was performed. The formulation of the electroplating solution is listed in the ESI† (Table S1). The applied current density was 10 mA cm<sup>-2</sup>; the electroplating time was controlled between 5–30 minutes to adjust the thickness of the Cu layer.

### Characterizations

The sheet resistance of the copper layer was measured by the four-point-probe method with a resistance analyzer (LorestaGP T610, Mitsubishi Chemical Analytech Co. Ltd). The tape peeling test was conducted as follows: Scotch tape (3M, USA) was firmly attached onto the surface of the circuit sample and then quickly peeled off in a vertical-to-film direction. Optical microscopic images were taken on a metallographic microscope (Olympus GX 51). The SEM-EDS analysis was conducted on an FEI Nova NanoSEM450 electron microscope. The differential scanning calorimetry and thermal gravimetric analyses (DSC-TGA) of the paste were taken with a NETZSCH STA449 F3 analyzer. The Fourier Transform Infrared Spectroscopy (FTIR) analysis was taken on a NICOLET iS50 FTIR spectrometer. The aging test of the copper conductive pattern was performed in a testing chamber at 85 °C and 85 relative humidity (RH) for 500 hours and the thermal shock test was taken at a cycling temperature from -40 °C to 125 °C for 500 cycles (90 minutes for each cycle).

## Results and discussion

Fig. 1 shows the schematic of the Cu galvanic replacement deposition process. Briefly, it requires three steps to create highly conductive Cu conductive patterns: firstly the Zn paste is screen printed on the substrate in the desired pattern, where the epoxy resin contained in the paste acts as both the binder and adhesive. Secondly, after the Zn paste is cured, the sample is immersed in the Cu<sup>2+</sup> ion solution, where the replacement

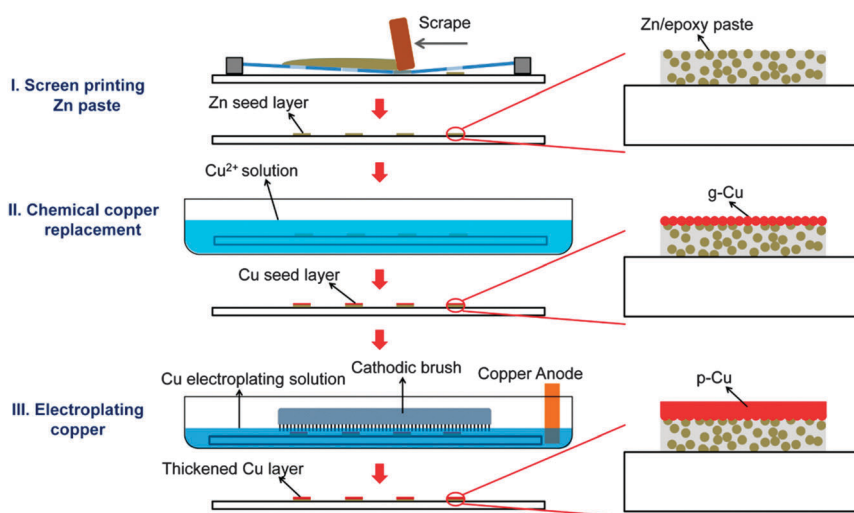


Fig. 1 Schematic of the fabrication process.

reaction takes place. The Cu<sup>2+</sup> ions can be reduced into a layer of Cu by Zn and deposited on the surface of the Zn paste layer; some of the copper is embedded into the voids resulting from the elimination of Zn filler particles. The deposited Cu particles interconnect and form a continuous Cu thin layer (a deposited Cu layer by galvanic replacement, marked as g-Cu) which is electrically conductive. Thirdly, a Cu electro-plating process is adopted to thicken the copper layer so that we can obtain a robust and stable Cu metal conductive layer (which includes both the Cu layer from galvanic replacement deposition and Cu layer from electro-plating deposition, marked as p-Cu) which is mechanically interlocked on top of the Zn-epoxy film with excellent conductivity. As shown in this figure, a cathodic brush made of stainless steel wires is used to ensure the electrical contact of every single trace.

Fig. 2 presents the morphology of the printed pattern in each step. From Fig. 2(a) and (b), we can observe that after the Zn paste is cured; the Zn particles are uniformly distributed on the surface, which provides an effective template for the subsequent g-Cu deposition; Fig. 2(c) and (d) show the *in situ* reduced g-Cu layer capping on the Zn paste and interconnecting into a percolation network. This continuous g-Cu thin layer shows a resistivity of  $\sim 4 \times 10^{-4} \Omega \text{ cm}$ , which is enough for electro-plating Cu. Fig. 2(e) and (f) show that the electro-plating deposited Cu (p-Cu) crystals form a uniform p-Cu film, the thickness of which can be adjusted by controlling the deposition time. In this way, we can obtain a highly conductive pure bulk copper (p-Cu) layer with a controllable thickness (5–30  $\mu\text{m}$ ) (see ESI† for details).

The formation of the g-Cu can be described by the following equation:  $\text{Zn} + \text{Cu}^{2+} \rightarrow \text{Zn}^{2+} + \text{Cu}$ , which is a simple spontaneous galvanic reaction between Zn seeds and the target metal Cu<sup>2+</sup> ions. Thus, it needs no catalyst or extra reducing agent, and the reaction can take place immediately at room temperature when immersing the printed Zn seed paste into the Cu<sup>2+</sup> ion solution. It should be noted, some additives (H<sub>2</sub>SO<sub>4</sub> and PEG) are needed to control the deposition kinetics by adjusting the pH value and

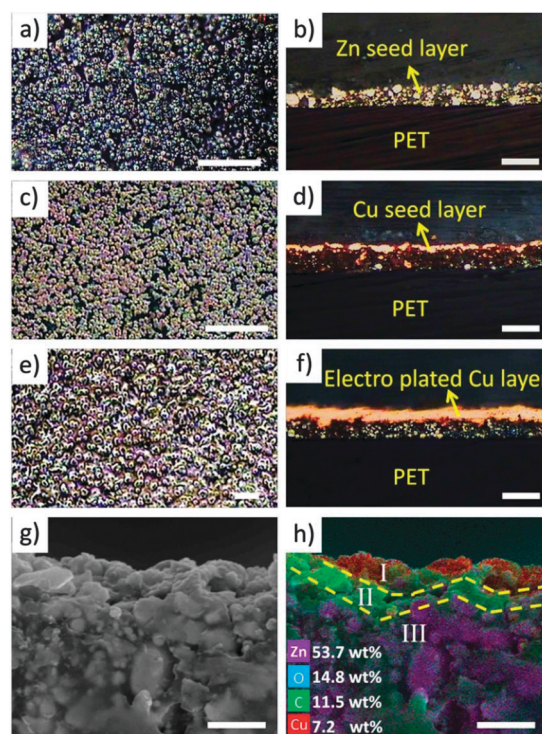


Fig. 2 Optical microscopic images of (a) top view of printed Zn paste pattern; (b) cross section of Zn pasted pattern; (c) top view of Zn paste covered with a thin Cu layer by replacement deposition (g-Cu); (d) cross section of the Zn paste covered with a thin Cu layer by galvanic replacement (g-Cu); (e) top view of the Cu layer after electro-plating (p-Cu) for 20 min for the sample in (c); (f) cross section of the Cu layer after electro-plating (p-Cu) for 20 min for the sample in (c); and SEM images of (g) the cross section of the Zn paste covered with g-Cu; (h) the EDS mapping of (g). The scale bars of (a), (c) and (e) are 50  $\mu\text{m}$ ; the scale bars of (b), (d) and (f) are 20  $\mu\text{m}$ ; the scale bars of (g) and (h) are 5  $\mu\text{m}$ .

the concentration of the surfactant, so that the deposited Cu can form a uniform thin layer (see ESI† for details: the Cu<sup>2+</sup> solution components). Since the Cu<sup>2+</sup> ion solution is acidic, Zn<sup>2+</sup> can be

easily dissolved. In this way, we can avoid the use of the expensive and environmentally unfriendly palladium (Pd) catalyst and the organic reducing agent that are used in conventional processes; and the  $\text{Cu}^{2+}$ - $\text{Zn}^{2+}$ - $\text{SO}_4^{2-}$ -PEG waste solution can be conveniently recycled. Fig. 2(f) and (g) present the elemental distribution of the sample cross sections of Cu wires after the replacement deposition. From Fig. 2(h), we can observe that in the surface layer which is marked as area I, the element is dominated by Cu, while in the bottom layer which is marked as area III, the elemental composition is C, O, and Zn which refers to the original Zn-epoxy paste. In the middle layer, which is marked as area II, there is much less Zn than in area III, indicating that the Zn in area II has mostly been replaced by Cu.

A strong bonding strength is a basic requirement for fine circuits. The adhesion between the p-Cu layer and the PET substrate was evaluated with the tape peeling test as shown in Fig. 3. Straight and parallel p-Cu circuit lines (200  $\mu\text{m}$  in width and distance) remained intact after we peeled off the tape, and nothing remained attached on the tape, indicating the strong mechanical strength of both the p-Cu layer itself and the interfaces between the p-Cu layer, the Zn-epoxy paste and the substrate. This result suggests the excellent robustness of the continuous p-Cu layer. Meanwhile, the mechanical interlocking effect of the rough interface surface between the p-Cu layer and the epoxy resin guarantees the adhesion force between them<sup>39</sup> (see ESI† for details). Besides, the oxygen-containing functional groups, such as C-O and C=O, on the surface of the epoxy resin may potentially interact with the p-Cu metal and thus further reinforce the interfacial bonding as well<sup>40–43</sup> (see ESI† for details: FTIR analysis). Therefore, the Zn-epoxy paste layer plays an important role in enhancing the adhesion between the metal and the polymer substrate.

The p-Cu conductive patterns fabricated on flexible substrates are highly flexible and foldable. For example, Fig. 4(c) shows that p-Cu circuits fabricated on a PET film can be

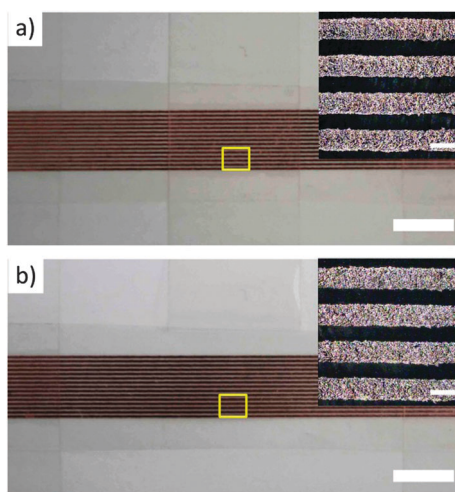


Fig. 3 Tape peeling test of the Cu circuits. (a) Before peeling (Scotch tape is adhered on top). (b) After peeling. The insets are optical microscope images of the selected area. The scale bars of (a) and (b) are 5 mm. The scale bars of the insets are 200  $\mu\text{m}$ .

wrapped around a glass stick (with a diameter of 8 mm) while the integrated light-emitting diodes (LEDs) still emit blue light; furthermore, even when we knot the p-Cu conductive circuits and fold the creases as shown in Fig. 4(d), the LEDs still work very well. In order to systematically evaluate the flexibility and foldability, a series of tests were conducted with the p-Cu circuits (5 cm  $\times$  1 mm) printed on PET (75  $\mu\text{m}$  in thickness). In the bending tests, the circuits were bent at different radii of curvature for 1000 cycles and each cycle comprised one stretching and compressing of the p-Cu circuits as shown in Fig. 4(a). Meanwhile, their resistance upon bending cycles was measured. The results were normalized as  $R/R_0$  vs. bending cycles as shown in Fig. 4(a), of which  $R$  is the resistance of the p-Cu circuits after bending and  $R_0$  is the resistance before the bending tests. It showed that when the p-Cu circuits were bent at a radius of 7.5 mm and 12 mm,  $R/R_0$  remained stable after 1000 cycles. When the bending radius decreased to below 5 mm,  $R/R_0$  increased to different extents. In general, the electrical resistance of the sample increased at the smaller bending radius, and after 1000 cycles  $R/R_0$  increased gradually to about 2, 3.3 and 6.5 at radii of 5 mm, 2 mm and 1 mm, respectively. This is because when the p-Cu circuits are repeatedly bent, material damage such as fatigue cracks tend to occur and accumulate with the bending cycles. Smaller bending radii result in more severe deformation and larger stress that cause more cracks and faster fatigue of the p-Cu layer.<sup>44</sup> In spite of the resistance increase, a  $\sim 6.5$ -fold greater  $R_0$  means a low electrical resistivity of  $\sim 10^{-5}$   $\Omega$  cm in the  $r = 1$  mm case, which

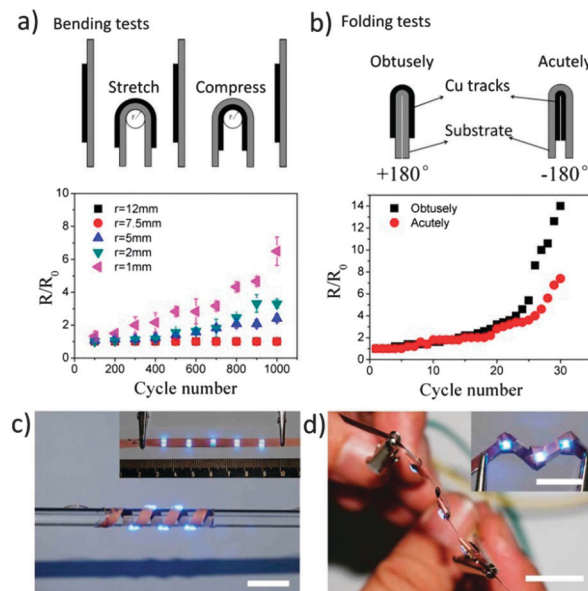


Fig. 4 Flexibility and foldability test results of the p-Cu circuits on PET substrate. (a) Top: Scheme showing the bending test of the p-Cu circuits. Bottom: Normalized resistance of the Cu circuits vs. bending cycles. (b) Top: Scheme showing the folding test of the p-Cu circuits. Bottom: Normalized resistance of the p-Cu circuits vs. folding cycles. (c) The p-Cu conductive tracks integrated with blue LEDs are conformally wrapped around a glass stick. Inset: Unwrapped p-Cu conductive tracks integrated with blue LEDs. The LEDs are turned on. (d) The side view of the knotted p-Cu tracks integrated with blue LEDs, the creases are folded. Inset: Top view of the knotted p-Cu tracks. The LEDs are turned on. The scale bars are 2 cm.

is applicable for a lot of flexible electronics applications. In the folding tests, the foldability of the p-Cu circuits was evaluated by measuring the resistance while folding the samples acutely ( $-180^\circ$ ) and obtusely ( $+180^\circ$ ), as depicted in Fig. 4(b). For both folding types, the resistance increased slowly in the first 15–20 cycles, of which  $R/R_0$  was 2.8 for the obtuse type and 2.2 for the acute type after 20 cycles. More drastic resistance increases were found after more bending cycle tests. Besides, the obtuse type showed a faster fatigue than the acute one, indicating that the tensile stress caused more serious damage to the p-Cu film, which was related to the thickness of the substrates as discussed in the previous reports.<sup>44,45</sup> Similar to the bending tests, folding the p-Cu circuits caused severe deformation and stress in the p-Cu layer resulted in fatigue and even failure of the p-Cu circuits. Also, the excellent foldability of the p-Cu circuits ensures reliable performance for applications in harsh working conditions.

Furthermore, accelerated aging tests were performed to evaluate the reliability of the p-Cu circuits when used in harsh working environments. The electrical resistance of the sample remained unchanged after being aged in an 85 °C/85 RH environment for 500 hours (ESI,† Fig. S11); no indication that an increase of electrical resistance of the sample was found after the sample was aged for 500 cycles of temperature variation between  $-40^\circ\text{C}$  and  $125^\circ\text{C}$  (ESI,† Fig. S12). The excellent aging reliability performance shown in the tests is mainly due to the stable physical and chemical property of the epoxy resin and bulk copper wires, and the fracture toughness and tensile strength of the p-Cu layer, which is even comparable to the conventional copper-clad plated products.

As can be seen, the introduction of epoxy resin plays an important role in this technology; firstly, it enables adequate printing of the Zn seed paste for the screen printing process; secondly, the cured epoxy resin has excellent adhesion strength

with many kinds of substrate materials, which serves as a binder. Finally, it provides a strong mechanical interconnection to the p-Cu layer, which guarantees excellent reliability of the p-Cu circuits. Overall, the current technology is simple and can be conveniently reproduced.

We have demonstrated a simple, additive, and Pd-free technology for wiring highly conductive Cu circuits, which is based on inexpensive materials and cost-effective processes. Because of the excellent process compatibility to screen printing and electroplating processes, this technology is promising for large scale and roll-to-roll fabrication. By our method, we can conveniently achieve a printing resolution down to 100  $\mu\text{m}$  (Fig. 5(a)), which satisfies the basic requirements for various applications, such as RFID tags, touch pads, and some flexible integrated circuits boards as shown in Fig. 5(b). This wiring resolution is comparable to the best case for conventional lithographic wiring resolution. Through properly adjusting the rheology of the Zn paste, we can integrate some other printing techniques to our current process, such as gravure printing, transfer printing and offset printing, which shows even better printing resolution and cost-effectiveness. We can also fabricate volumetric circuits conveniently by pad printing on a non-planer surface, as shown in Fig. 5(c), which may potentially find advanced radio frequency applications *etc.*<sup>46,47</sup>

Fig. 5(d)–(f) present the RFID samples with the antennas fabricated by different methods. It was found that the electrical resistance of the p-Cu pattern that was fabricated by our technology is similar to that of the commercial aluminium (Al) antenna, and is about 26 times smaller than that of the Ag paste (75 wt% of Ag loading) based antenna. In this case, the reading/writing distance for p-Cu RFID is about 3.5 m, similar to the commercial Al one, while the Ag conductive adhesive based antenna only has a reading/writing distance of 1.8 m (details are shown in ESI,† Table S2). The excellent performance

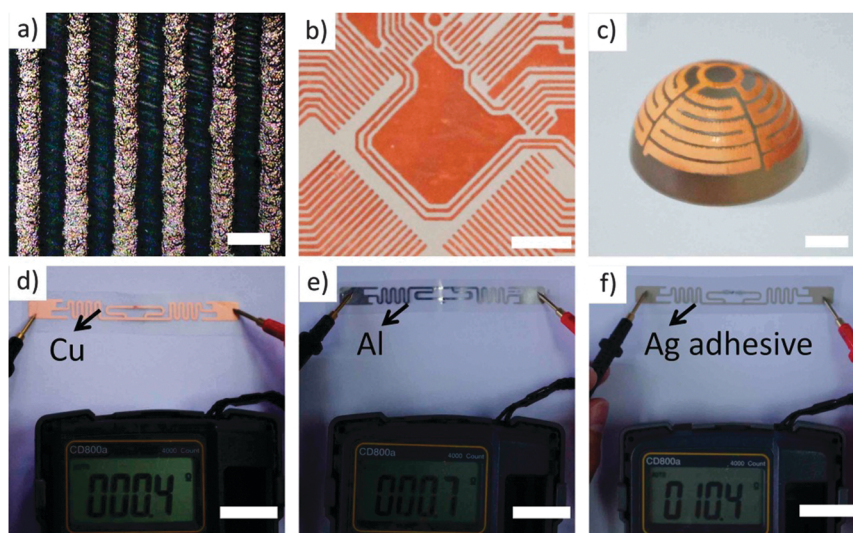


**Fig. 5** Circuits made by replacement deposition of Cu. (a) Optical microscope image of circuits of width 100  $\mu\text{m}$  after electroplating Cu. (b) Part of the electronic circuit, the minimum line width is 200  $\mu\text{m}$ . (c) A volumetric antenna prepared by the involvement of pad printing. (d) A piece of UHF-RFID antenna sample fabricated with p-Cu. (e) A commercial UHF-RFID antenna sample fabricated with Al. (f) A piece of UHF-RFID antenna sample fabricated with Ag paste. The scale bar of (a) is 200  $\mu\text{m}$ ; the scale bar of (b) and (c) is 5 mm; the scale bars of (d)–(f) are 20 mm.

of the p-Cu based RFID shown in the tests is mainly due to its high conductivity, which is beneficial to reduce signal losses. Therefore, the highly conductive p-Cu circuits fabricated by our technology result in the low cost and high performance materials required for potential electronic device applications.

## Concluding remarks and outlook

In summary, we have developed a simple technology combining galvanic replacement and electro-plating processes on Zn seed paste. This simple additive process can lead to the fabrication of high quality conductive Cu wires. The Zn paste that we developed is compatible with various efficient printing techniques, and is simple and inexpensive. Through evaluating the performance and fabricating prototypes, we have demonstrated that the fabricated p-Cu circuits have superior conductivity and reliable performances, which may find immediate electronics applications, such as flexible circuit boards, RFID tags, touch panels, membrane switches, photovoltaics and others.

What's more, following our methodology, this technology can be extended to the applications of other seed and conductive materials: for example, using iron and nickel *etc.* as the seed metals and using Ag or Au *etc.* to replace Cu as the conductive materials. Therefore, in this case study, we have proposed a simple and easy-to-operate technology for fabricating a wide range of high performance electronic circuits.

## Acknowledgements

This work is financially supported by Shenzhen Technical Project CYJ2013-0402145002411, the National Key Basic Research (973) Program (2014CB932400), Guangdong Province Innovation R&D Team Plan No. 2009010025, and National Nature Science Foundation of China No. 51202120 and 51232005.

## Notes and references

- 1 S. W. Hwang, X. Huang, J. H. Seo, J. K. Song, S. Kim, S. Hage Ali, H. J. Chung, H. Tao, F. G. Omenetto and Z. Ma, *Adv. Mater.*, 2013, **25**, 3526–3531.
- 2 Z. Li, T. Le, Z. Wu, Y. Yao, L. Li, M. Tentzeris, K. S. Moon and C. Wong, *Adv. Funct. Mater.*, 2015, **25**, 464–470.
- 3 S. W. Hwang, J. K. Song, X. Huang, H. Cheng, S. K. Kang, B. H. Kim, J. H. Kim, S. Yu, Y. Huang and J. A. Rogers, *Adv. Mater.*, 2014, **26**, 3905–3911.
- 4 R. C. Webb, A. P. Bonifas, A. Behnaz, Y. Zhang, K. J. Yu, H. Cheng, M. Shi, Z. Bian, Z. Liu and Y.-S. Kim, *Nat. Mater.*, 2013, **12**, 938–944.
- 5 W. H. Yeo, Y. S. Kim, J. Lee, A. Ameen, L. Shi, M. Li, S. Wang, R. Ma, S. H. Jin and Z. Kang, *Adv. Mater.*, 2013, **25**, 2773–2778.
- 6 W. Honda, S. Harada, T. Arie, S. Akita and K. Takei, *Adv. Funct. Mater.*, 2014, **24**, 3299–3304.
- 7 M. Song, D. S. You, K. Lim, S. Park, S. Jung, C. S. Kim, D. H. Kim, D. G. Kim, J. K. Kim and J. Park, *Adv. Funct. Mater.*, 2013, **23**, 4177–4184.
- 8 J. Yeo, G. Kim, S. Hong, M. S. Kim, D. Kim, J. Lee, H. B. Lee, J. Kwon, Y. D. Suh and H. W. Kang, *J. Power Sources*, 2014, **246**, 562–568.
- 9 W. Shen, X. Zhang, Q. Huang, Q. Xu and W. Song, *Nanoscale*, 2014, **6**, 1622–1628.
- 10 M. Liu, J. Wang, M. He, L. Wang, F. Li, L. Jiang and Y. Song, *ACS Appl. Mater. Interfaces*, 2014, **6**, 13344–13348.
- 11 W. Wu, S. Yang, S. Zhang, H. Zhang and C. Jiang, *J. Colloid Interface Sci.*, 2014, **427**, 15–19.
- 12 K. Jost, D. Stenger, C. R. Perez, J. K. McDonough, K. Lian, Y. Gogotsi and G. Dion, *Energy Environ. Sci.*, 2013, **6**, 2698–2705.
- 13 D. A. Alsaïd, E. Rebrosova, M. Joyce, M. Rebroso, M. Atashbar and B. Bazuin, *J. Disp. Technol.*, 2012, **8**, 391–396.
- 14 G. Hernandez-Sosa, S. Tekoglu, S. Stolz, R. Eckstein, C. Teusch, J. Trapp, U. Lemmer, M. Hamburger and N. Mechau, *Adv. Mater.*, 2014, **26**, 3235–3240.
- 15 A. Carlson, S. Wang, P. Elvikis, P. M. Ferreira, Y. Huang and J. A. Rogers, *Adv. Funct. Mater.*, 2012, **22**, 4476–4484.
- 16 T.-I. Kim, M. J. Kim, Y. H. Jung, H. Jang, C. Dagdeviren, H. A. Pao, S. J. Cho, A. Carlson, K. J. Yu and A. Ameen, *Chem. Mater.*, 2014, **26**, 3502–3507.
- 17 C. H. Lee, D. R. Kim and X. Zheng, *Nano Lett.*, 2011, **11**, 3435–3439.
- 18 A. Tabatabai, A. Fassler, C. Usiak and C. Majidi, *Langmuir*, 2013, **29**, 6194–6200.
- 19 J. T. Muth, D. M. Vogt, R. L. Truby, Y. Mengüç, D. B. Kolesky, R. J. Wood and J. A. Lewis, *Adv. Mater.*, 2014, **26**, 6307–6312.
- 20 Y. Zheng, Z. Z. He, Y. X. Gao and J. Liu, *Sci. Rep.*, 2013, **3**, 1786.
- 21 J. La Dou, *Int. J. Hyg. Environ. Health*, 2006, **209**, 211–219.
- 22 J. Liu, C. Yang, H. Wu, Z. Lin, Z. Zhang, R. Wang, B. Li, F. Kang, L. Shi and C. P. Wong, *Energy Environ. Sci.*, 2014, **7**, 3674–3682.
- 23 J. Perelaer, R. Abbel, S. Wunscher, R. Jani, T. van Lammeren and U. S. Schubert, *Adv. Mater.*, 2012, **24**, 2620–2625.
- 24 S. Jeong, S. H. Lee, Y. Jo, S. S. Lee, Y. H. Seo, B. W. Ahn, G. Kim, G. E. Jang, J. U. Park, B. H. Ryu and Y. Choi, *J. Mater. Chem. C*, 2013, **1**, 2704–2710.
- 25 D. Tobjork and R. Osterbacka, *Adv. Mater.*, 2011, **23**, 1935–1961.
- 26 C. Yang, C. P. Wong and M. M. Yuen, *J. Mater. Chem. C*, 2013, **1**, 4052–4069.
- 27 Y. Lee, J. R. Choi, K. J. Lee, N. E. Stott and D. Kim, *Nanotechnology*, 2008, **19**, 415604.
- 28 J. Perelaer, R. Jani, M. Grouchko, A. Kamyshny, S. Magdassi and U. S. Schubert, *Adv. Mater.*, 2012, **24**, 3993–3998.
- 29 D. Angmo, T. T. Larsen-Olsen, M. Jørgensen, R. R. Sondergaard and F. C. Krebs, *Adv. Energy Mater.*, 2013, **3**, 172–175.
- 30 W.-H. Chung, H.-J. Hwang, S.-H. Lee and H.-S. Kim, *Nanotechnology*, 2013, **24**, 035202.
- 31 K. Cheng, M. H. Yang, W. W. Chiu, C. Y. Huang, J. Chang, T. F. Ying and Y. Yang, *Macromol. Rapid Commun.*, 2005, **26**, 247–264.

- 32 P. C. Hidber, W. Helbig, E. Kim and G. M. Whitesides, *Langmuir*, 1996, **12**, 1375–1380.
- 33 D. Zabetakis and W. J. Dressick, *ACS Appl. Mater. Interfaces*, 2012, **4**, 2358–2368.
- 34 M. Charbonnier, M. Romand, Y. Goepfert, D. Leonard and M. Bouadi, *Surf. Coat. Technol.*, 2006, **200**, 5478–5486.
- 35 Y.-C. Liao and Z.-K. Kao, *ACS Appl. Mater. Interfaces*, 2012, **4**, 5109–5113.
- 36 S. Ma, L. Liu, V. Bromberg and T. J. Singler, *ACS Appl. Mater. Interfaces*, 2014, **6**, 19494–19498.
- 37 P. Zhu, Y. Masuda and K. Koumoto, *J. Mater. Chem.*, 2004, **14**, 976–981.
- 38 Y. Chang, C. Yang, X.-Y. Zheng, D.-Y. Wang and Z.-G. Yang, *ACS Appl. Mater. Interfaces*, 2014, **6**, 768–772.
- 39 K. Cho and E. C. Cho, *J. Adhes. Sci. Technol.*, 2000, **14**, 1333–1353.
- 40 C. K. Y. Wong, M. M. F. Yuen and B. Xu, *Appl. Phys. Lett.*, 2009, **94**, 263102.
- 41 W. J. Lee, Y. S. Lee, S. K. Rha, Y. J. Lee, K. Y. Lim, Y. D. Chung and C. N. Whang, *Appl. Surf. Sci.*, 2003, **205**, 128–136.
- 42 C. Wang, L. Xiang, Y. Chen, S. Wang, D. Xiao and W. He, *J. Adhes. Sci. Technol.*, 2015, 1–12.
- 43 W.-J. Liu, X.-J. Guo and C.-H. Chuang, *Surf. Coat. Technol.*, 2005, **196**, 192–197.
- 44 R. S. Guo, Y. Yu, Z. Xie, X. Q. Liu, X. C. Zhou, Y. F. Gao, Z. L. Liu, F. Zhou, Y. Yang and Z. J. Zheng, *Adv. Mater.*, 2013, **25**, 3343–3350.
- 45 H. Y. Wu, S. W. Chiang, W. Lin, C. Yang, Z. Li, J. P. Liu, X. Y. Cui, F. Y. Kang and C. P. Wong, *Sci. Rep.*, 2014, **4**, 6275.
- 46 J. J. Adams, E. B. Duoss, T. F. Malkowski, M. J. Motala, B. Y. Ahn, R. G. Nuzzo, J. T. Bernhard and J. A. Lewis, *Adv. Mater.*, 2011, **23**, 1335–1340.
- 47 C. Pfeiffer, X. Xu, S. R. Forrest and A. Grbic, *Adv. Mater.*, 2012, **24**, 1166–1170.